RSC Advances

ROYAL SOCIETY OF CHEMISTRY

www.rsc.org/advances

Thermally stable phthalonitrile resins based on multiple oligo (aryl ether)s with phenyl-*s*-triazine moieties in backbones

Lishuai Zong, Cheng Liu, Shouhai Zhang, Jinyan Wang*, and Xigao Jian

State Key Laboratory of Fine Chemicals, Department of Polymer Science and Materials, School of Chemical Engineering, Dalian University of Technology, Dalian 116024, China

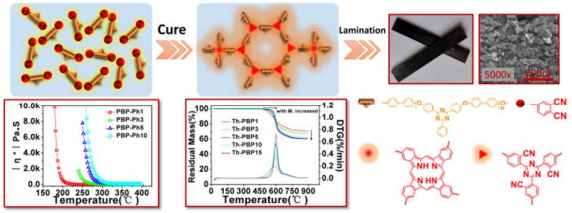

Phenyl-*s*-triazine segments in backbones would endow phthalonitrile networks enhanced thermal stabilities, which could also be tuned by the aromatic ether main-chain lengths.

RSC Advances

ARTICLE

Thermally stable phthalonitrile resins based on multiple oligo (aryl ether)s with phenyl-*s*-triazine moieties in backbones†

Received 00th January 20xx,
Accepted 00th January 20xx

DOI: 10.1039/x0xx00000x

www.rsc.org/

Lishuai Zong,[a] Cheng Liu,[a] Yujie Guo,[a] Jinyan Wang,*[a] and Xigao Jian[a]

Many efforts have been devoted to tailoring the architecture of phthalonitrile (PN) polymers in recent years. Herein, we disclose a series of novel PN oligomers (PBP-Phs) bearing heteroaromatic phenyl-*s*-triazine moieties, serving as thermally stable segments, in backbones. With bis(4-[4-aminophenoxy]phenyl)sulfone as curing additive, PBP-Phs displayed commendable processability. After cured at high temperatures (up to 375 °C), the resulting networks (Th-PBPs) exhibit high glass transition temperatures ranging from 294 °C to 400 °C and outstanding thermal stability with weight retention of 95% in N_2 lying between 538 °C and 582 °C, the overall thermal properties which, are in close connection with the oligomer molar weights. Additionally, the feasibility of Th-PBPs reinforced with unidirectional continuous carbon fibers (CF) was evaluated. The results show that CF/Th-PBP laminates possess high flexural strength (1339-1855 MPa) and interlaminar shear strength (71.8-92.2 MPa).

Introduction

The development of novel high-performance materials is one of the urgent challenges facing aerospace industry in the last few decades.[1] More recently, an increasingly requirement of these materials and their composites for heat-resistance components used in aerospace vehicles such as the space shuttle and reentry module has been emerging. Among sorts of high-performance materials,[2] phthalonitrile (PN) resins[3] are supposed to meet the harsh application condition because of possessing unique combined properties, *e.g.*, facile preparation, excellent thermal properties, superior flame and chemical resistance, and less flaming smog.[4]

In 1958, Marvel and coworkers have first disclosed the study on PNs in terms of thermally stable materials,[5] but these works had not aroused wide interest of researchers, mainly due to their harsh curing condition.[6] Keller and coworkers found that primary amines could accelerate the polymerization of PN precursors to give more stable thermosets.[7] Afterwards, this type of additives have been deemed having obviously advantageous over other curing additives such as metals,[8] metallic salts,[9] organic acids,[4c] phenols,[10] amines,[11] and bispropargyl ether.[12] Two factors have been considered. First, robust interaction between amines and PNs could lead to a higher degree of polymerization, consequently generating a more thermally stable thermoset.[7b, 11a] Second, the amine-motivated curing reaction is much easier to control by tailoring the amine type and concentration as well as varying the curing temperature, which could enable PN resins to adjust those more cost-effective processing methods such as resin transfer molding (RTM), resin infusion molding (RIM), and vacuum-assisted resin transfer molding (VARTM).[13]

On the other hand, a rational design on the architecture of PN polymers has been taken into account by many researchers. First-generation PN resins, derived from low molecular weight PN monomers, are generally associated with high glass transition temperature (T_g, >400 °C) and 5% mass loss temperature ($T_{d5\%}$, >500 °C), due to a high cross-linking density originated from a short structural unit between the cross-linking sites, phthalocyanine or *s*-triazine moieties.[14] Accordingly, self-catalyzed[3d, 14b, 15] and tri-functional[11b] PN monomers, which would lead to much higher cross-linking density networks, were synthesized, resulting in ultra-high T_gs. Nevertheless, these resins would inevitably suffer from brittle weakness, also stemmed from their high cross-linking density. Second-generation PN resins, featuring various oligomeric aromatic ether spacers between the cross-linking sites, have provided an alternative way to overwhelm this drawback. In this sense, PN resins with versatile structures have been developed.[4a, 4f, 16] Lately, the Naval Research Laboratory (NRL) has achieved the certification of PEEK-based PN resins and composites for commercial applications, manifesting the superiority of second-generation PN resins. Their attractive properties made them suitable for advanced technological applications including composites,[17] adhesives, electronic conductors,[18] magnetic and microwave absorption materials.[4d, 19] However, there are few efforts devoted to modifying PN polymer properties with

[a] State Key Laboratory of Fine Chemicals, Department of Polymer Science and Materials, School of Chemical Engineering, Dalian University of Technology, Dalian 116024, China E-mail: wangjinyan@dlut.edu.cn; Tel: +86-411-84986109

† Electronic Supplementary Information (ESI) available: Six figures and three tables, including the FTIR spectra, NMR spectra, parameters of rheologic property, thermal data, SEM images as well as the T_g and $T_{d5\%}$ comparison data.. See DOI: 10.1039/x0xx00000x

thermally stable and high-stiff moieties.[20] Such groups would plausibly enhance the polymer structure integrity, in turn to drive an improvement of polymer heat-resistance.

Motivated by this concept, our group introduced the twisted, non-coplanar phthalazinone group to build novel PN precursors,[21] subsequently discussing their polymerization to phthalocyanine or *s*-triazine networks and properties. Herein, we furthered this concept to incorporate phenyl-*s*-triazine unit in polymer backbones. The presence of *s*-triazine unit would enhance the rigidity of the polymer backbone due to the strong charge transfer interaction between the *s*-triazine ring and aromatic ring.[22] Based on the literatures, the phenyl-*s*-triazine-containing monomers, namely 2-phenyl-4,4-bis(4-fluorophenyl) -1,3,5-triazine (BFPT), could be synthesized *via* a three-step or four-step route. However, both of these approaches suffer from toxic and irritant smelling SO_3 or NH_3 and especially low yield.[23] Our previous work presented a facile one-step synthetic strategy to produce BFPT with high yield (>80%),[24] which would guarantee plenteous BFPT for immense employment. In this work, we designed and prepared a series of phenyl-*s*-triazine-containing PN oligomers with multiple aromatic ether chains in backbones (Scheme 1), named as PBP-Phn. *n* represents the designed value of the repeating unit of the oligomer, and was controlled by the monomer feed ratios. Bis[4-(4-aminophenoxy)phenyl]sulfone (BAPS, 5 wt %) was selected to co-cure with PBP-Phs. The melting behaviour of PBP-Ph/BAPS blends was concerned and the properties (*i.e.* thermal and thermo-oxidative stability, water absorption capacity, thermal property, and mechanical property) of the cured networks (Th-PBPs) or their advanced CF composite laminates (CF/Th-PBPs) were investigated as well.

Experimental

Materials

4,4'-Biphenol (BP, 99%) were purchased from Haiqu chemical Co., shanghai, China. 4-Fluoro-benzonitrile (FBN, 99%) and 4-nitro-phthalonitrile (NPh, 99%) were purchased from Jiakailong chemical Co., Wuhan, China. Benzaldehyde (BA, A.R.), chlorobenzene (CB, A.R.), toluene (A.R.) and other solvents were purchased from Kermel Chemical Reagent Co., Ltd., Tianjin, China. All chemicals and solvents above were used without further purification. Anhydrous potassium carbonate (K_2CO_3, 99%, Beijing Chemical Co., China.) was ground and dried in vacuum at 100 °C for 24 h before utilized. N-methyl pyrrolidone (NMP, A.R., Kermel Chemical Reagent Co., Ltd.) was refluxed with CaH_2 for 2 h, and then vacuum distilled. The 125-127 °C boiling range fraction was collected and stored over molecular sieves (type 4Å). T300 CF fabric was provided by Aviation Industry Corporation of China (AVIC). T700 continuous CF was purchased from TORAY and disposed at 350 °C for 5-10 min before used.

Bis[4-(4-aminophenoxy)phenyl]sulfone (BAPS) was prepared according to described work by Barikani.[25] Purity: 99 wt %. APCI/MS (M+ Calcd. as $C_{21}H_{13}N_2F_2$: m/z=432.11): m/z=432.00 (M+).

2-Phenyl-4,6-bis(4-fluorophenyl)-1,3,5-triazine was facilely prepared *via* a one-step route based on our previous work.[24] M.p.: 260.2-260.8 °C; purity: 99 wt %. MALDI-TOF/MS (M+ Calcd. as $C_{21}H_{13}N_2F_2$ 345.1078): m/z=345.1067(M+). ^{1}H-NMR (400M, $CDCl_3$): δ 8.91-8.61 (m, 6H), 7.74-7.50 (m, 3H), 7.39-7.12 (m, 4H).

Methods and equipment

High Performance Liquid Cromatography (HPLC) was conducted on a Hewlett-Packard (HP) 1100 liquid chromatograph. Inherent viscosities (η_{inh}) of the polymers were tested using an Ubbelohde capillary viscometer at a concentration of 0.5 gd/L in NMP at 25 °C. Fourier transform infrared (FT-IR) measurements were performed with a Thermo Nicolet Nexus 470 FT-IR spectrometer. ^{1}H-NMR (400 MHz) and ^{13}C-NMR (100 MHz) spectra were recorded on a Varian Unity Inova 400 spectrometer using $CDCl_3$ and CF_3COOD mixed solvents. Matrix-assisted laser desorption ionization time-of-flight mass spectroscopy (MALDI-TOF-MS) analyses were performed on a Micromass GC-TOF CA 156 MALDI-TOF/MS. Gel permeation chromatography (GPC) analysis was carried out on an Agilent PL-GPC 50 Intergrated GPC system equipped with two PLgel 5 μm MIXED-C columns (300×7.5 mm) arranged in series with NMP as solvent calibrated with polystyrene standards. The solubility test was performed by dissolving 0.04g oligomer in 1mL solvent (4%, w/v) at different temperatures. Differential scanning calorimetry (DSC) were determined using a modulated TA Q20 instrument at a heating rate of 10 °C/min or 20 °C/min under a nitrogen flow of 50 mL/min. Thermal Gravimetric Analysis (TGA) was obtained from a TA Q500 instrument at a heating rate of 20 °C/min in N_2 or air. Gel contents of the cured samples were studied according to ASTM D2765-11 standard; NMP was selected as the extracting solvent. The water absorptions were obtained based on ASTM D570-98 standard. The resin content of the T700 reinforced composite was measured according to ASTM D3171-11 standard; *Annex A7* procedure was used to digest the matrices at 600 °C, and a paralleled sample of carbon fiber was heated simultaneously for calculating the original mass of the carbon fiber in the composite. SEM studies were performed on the cracked section of the composite with a FEI QUANTA 450 instrument at 15 kV.

Oligomer synthesis

PBP-Phs possessing multiple molar weights were prepared by a similar two-step one-pot reaction (Scheme 1). Their molecular weights were controlled by the reactant feed ratios (Table 1). Herein, the synthetic route of PBP-Ph5 was given as representative. To a 250 mL three-necked flask fitted with a Dean-Stark trap and a nitrogen inlet were charged BP (0.120 mol, 22.378 g), K_2CO_3 (0.160 mol, 22.114 g), 60 mL NMP and 60 mL toluene. The temperature was then raised gradually to 140 °C under a nitrogen atmosphere. The by-product water was removed by azeotroping with toluene. Then, the reaction was cooled to room temperature. BFPT (0.100 mol, 34.534g) along with 20 mL NMP was added into the flask. The system was heated stepwise to 190 °C, and maintained at this temperature for 6 h. The obtained solution was then cooled down at 50 °C.

NPh (0.022 mol, 3.809 g) and 20 mL NMP were added into the flask. The reaction system was heated to 80 °C for 8-10 h. After cooling to room temperature, the resultant brown mixture was poured to 5 % aqueous NaOH solution. The filtered solid was rinsed continuously with 5 % aqueous NaOH solution until the color of the filtrate faded away. Then the solid was washed with distilled water until neutral. Subsequently, the dried crude product was purified by reprecipitation from NMP into ethanol, and then dried at 120 °C in a vacuum oven for 24 h. Yield: 95 %. The characterization spectra for PBP-Phs with assignments are provided in Electronic Supplementary Material (Fig. S1-S4).

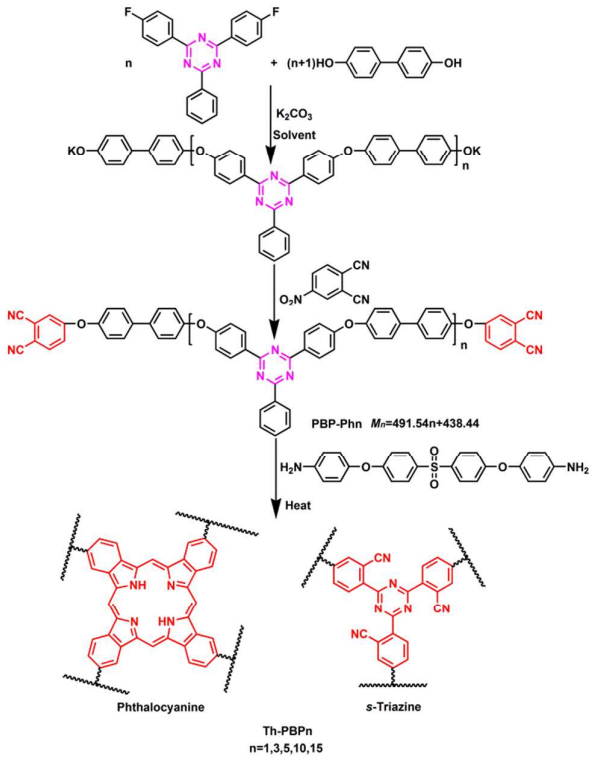

Scheme 1 Synthetic route of PBP-Phs and subsequent network Th-PBPs formation.

Curing procedure for Th-PBPs

All cured Th-PBPs were derived from their relative PBP-Phs with 5 wt % BAPS by an analogous procedure (Scheme 1). The typical curing procedure of Th-PBP5 was described as follows. 1.0 g PBP-Ph5 along with 0.05 g BAPS (5 wt %) was thoroughly grounded, and then compressed to a void-free flaky cylinder (Φ 25×2 mm^3) under elevated pressure. The sample was thermally cured by heating in an oven at 250 °C for 3 h, 285 °C for 1 h, 325 °C for 3 h, 350 °C for 2 h, and 375 °C for 8 h to afford the cross-linked polymer. Then, a portion of Th-PBP5 was powdered for DSC and TGA analysis, and the residual bulky sample was used for long-term oxidative stability and water-uptake studies.

Fabrication of CF/Th-PBP composite laminates

CF/Th-PBP composite laminates were fabricated *via* a parallel solution impregnation process (Fig. S5). The BAPS loading is 5 wt % of PBP-Phs. The CF/Th-PBP5 laminate was prepared using a three-step procedure as follows: (i) To a three-necked flask was charged 50 g PBP-Ph5, and then the flask was heated to 280 °C. 2.5 g BAPS was added to the molten PBP-Ph5 with vigorous stirring. The mixture was maintained at 280 °C for 5 min, and then cooled down. The obtained pre-polymer (B-stage resin) was dissolved in 100 mL NMP. (ii) The T700 carbon filament was dipped into the solution, and winded continuously to an iron frame of 300×210 mm^2 to afford the unidirectional prepreg. After dried under the infrared lamp, the prepreg was transferred to a vacuum oven, dried at 180 °C for 36 h, 200 °C for 1h. Then, the prepreg was tailored into 100×60 mm^2 dimension. (iii) Twelve tailored prepreg plies were stacked unidirectionally into a tight steel mould with a pressure of 2.5 MPa at 280 °C for 2 h. Then the steel mould was removed, and the obtained laminate was cured at 250 °C for 1 h, 285 °C for 1 h, 325 °C for 3 h, 350 °C for 2 h and 375 °C for 8 h in a muffle furnace. The dipping solution of PBP-Ph15 was prepared at room temperature without undergoing B-stage formation stage, owing to the infusibility of PBP-Ph15. Additionally, both the B-stage-resin generation and the laminating of PBP-Ph1 were performed at 250 °C, because this temperature is sufficient for processing. The thicknesses of all the finished laminates were approximately 2 mm. It should be sawed and sanded into 80×12.5×2 mm^3 size and 20×10×2 mm^3 size for flexural strength and interlaminar shear strength tests, respectively. The weight percentages of the fiber in the laminates were 62.7-69.2% based on the ASTM D3171-11 standard.

Rheological behaviour study

The samples for rheometric tests should be compressed into cylinder-shape flake with the dimension of Φ 25×1 mm^3 beforehand, and then a TA AR2000 instrument was used to study the rheological behaviours of the resins under a frequency of 1 Hz and a strain of 0.02 N.

Mechanical measurement

The flexural strength and interlaminar shear strength were determined using an Instron-5869 machine with a capacity of 500 N on T700 composite samples according to ASTM D790-11 and ISO 14130 standards, respectively.

Dynamic mechanical analysis (DMA) study

DMA measurements were conducted on a TA Q800 instrument at a frequency of 1 Hz and a heating rate of 3 °C/min from 25-400 °C with an air flow e using a 30×10×2 mm^3 T300/Th-PBP composite samples, in order to obtain the dynamic mechanical spectra including mechanical damping tan δ, storage modulus E' and loss modulus E". The fabrication procedure of T300/Th-PBP laminates are presented in Electronic Supplementary Material. The cross-sectional images of the laminates are shown in Fig. S6.

Oxidative stability measurements

0.5 g samples of all Th-PBPs were simultaneously handled in a muffle furnace and heated stepwise at various temperatures (250-450 °C) each for 8-h intervals under static air atmosphere.

The retention weights for every temperature step were recorded to determine the oxidative stabilities of Th-PBPs.

Results and discussion

Oligomer synthesis

To develop PN materials with advanced heat-resistant grade and to be employed in more extensive fields, the resins need to have a few key characteristics, including facile preparation, absence of by-products, tailorability, and appreciable processability. All these features would be encompassed in the PN resins based on the phenyl-*s*-triazine-bearing oligo (aryl ether)s, namely PBP-Phs. Specifically, oligomer PBP-Phs with multiple molecular weights were typically prepared in good yields by a one-pot method consisting of two nucleophilic substitution steps (scheme 1). The first step is the reaction between *s*-triazine-activated BFPT and bisphenol BP through a Meisenheimer complex at 190 °C. High boiling-point solvent NMP (202 °C) was adopted as the reaction media to allow for appropriate reacting temperature and sufficient solubility for the products. In the second step, the reaction underwent a milder nitro-substituted reaction at 80 °C for 8-10 h. An excess amount (5 %) of NPh was added to ensure complete conversion of phenolates into cross-linkable phthalonitrile moieties. The molecular weights of PBP-Phs were tuned by strictly controlling the feed ratios of BP versus BFPT as Table 1 shows. Afterwards, the M_ns of the resultant oligomers were simultaneously measured by GPC and the terminal analysis method[26] on their ^{1}H-NMR spectra, the values of which are in fair agreement with those expected as Table 1 shows.

Table 1 Synthetic data of PBP-Phs

Sample	Charge Ratio (BP:BFPT:NPh)	Temperature (°C)	Time (h)	M_n[a]	M_n[b]	M_n[c]	PD[b]	Yield(%)	η[d](dL/g)
PBP-Ph1	2:1:2.1	190	4	1316	1011	930	3.69	92	0.01
PBP-Ph3	4:3:2.1	190	4	1884	1758	1913	3.17	95	0.06
PBP-Ph5	6:5:2.1	190	4	4220	3836	2896	2.87	95	0.13
PBP-Ph10	11:10:2.1	190	6	4907	5175	5354	2.42	93	0.33
PBP-Ph15	16:15:2.1	190	6	7460	7528	7812	2.09	94	0.51

[a] Number-average molar mass calculated by the integration area of characteristic peaks through the ^{1}H-NMR spectra.
[b] Number-average molar mass and polydispersity measured by GPC in NMP calibrated with polystyrene standards.
[c] Number-average molar mass determined by feed ratios.
[d] Inherent viscosity determined at a concentration of 0.5 g/dL in NMP at 25 °C.

Solubility is a basic factor affecting the processing of resins. As expected, all PBP-Phs are readily soluble in NMP and tetrachlorethane (Table 2). This may be resulted from both the strongly polar phthalonitrile terminals and low molecular weights. As the main-chain length of the oligomer increases, the polarization of phthalonitrile units weakens due to their decreased contents, causing insoluble tendency in turn. Still, the rational solubility of PBP-Phs would substantially make them suitable for composite purpose *via* solution impregnating technology, which would undoubtedly extend their applications.

Table 2 Solubility of oligomer PBP-Phs[a]

Sample	NMP[b]	$C_2H_2Cl_4$	Py	$CHCl_3$	DMSO	DMAc	DMF	CB	Sf	THF	IP
PBP-Ph1	++	++	+	+-	+-	+-	+-	+-	+-	+-	-
PBP-Ph3	++	++	+	+-	+-	+-	+-	+-	+-	+-	-
PBP-Ph5	+	+	+-	+-	+-	+-	+-	+-	+-	+-	-
PBP-Ph10	+	+	+-	+-	-	+-	+-	+-	+-	+-	-
PBP-Ph15	+	++	+-	+-	-	+-	-	+	+-	+-	-

[a] Solubility: ++ soluble in room temperature; + soluble on heating; +- partially soluble on heating; - insoluble.
[b] NMP: N-methylpyrrolidone; Py: pyridine; DMSO: dimethylsulfoxide; DMAc: N,N-dimethyl acetamide; DMF: N,N-dimethyl formamide; CB: chlorobenzene; Sf: sulfolane; THF: tetrahydrofuran; IP: isopropanol.

Characterization

The structures of PBP-Phs were exactly characterized by the FT-IR (Fig. S1) and NMR (Fig. S2-S4) spectra, in which all peaks were well consistent with their intended chemical structure. The FT-IR spectra of PBP-Phs (Fig. S1) demonstrate the characteristic bands of *s*-triazine group at 1486 cm^{-1} and 1365 cm^{-1}. The stretching bands at 2230 cm^{-1} locate the cyano groups. Furthermore, the exact structures of PBP-Phs could be certified by the NMR spectra, and all the discernible shifting peaks in the ^{1}H-NMR spectra of PBP-Phs (Fig. S2) could be accurately assigned with the assistance of the ^{1}H-^{1}H gCOSY spectrum of PBP-Ph1 (Fig. S3). The set of peaks shifting downfield at 8.63-8.70 ppm are attributed to the protons (H5), which are adjacent to *s*-triazine groups, and the peaks at 8.48-8.54 ppm belong to H6 (Fig. S2). These signals can be used as the referenced signals to position the protons (H1-4, 7, 8). The rest protons resonating at 8.32-8.40 ppm are associated with H9, 10 of phthalonitrile moiety. Note that both the characteristic bands of nitrile group in Fig. S1 and the resonating signals of hydrogen protons (H9, 10, and 11) in Fig. S2 weaken with the increase of the molecular weights of PBP-Phs, indicative of the decreasing contents of the terminal nitrile groups. Additionally, the ^{13}C-NMR spectrum of PBP-Ph5 (Fig. S4) could also provide potent evidence for confirming its structure. The shifting signals at 159.9 and 164.4 ppm are assigned to the C18 and 19 in the phenyl-*s*-triazine groups. The

peaks at 130.1 and 129.9 ppm belong to the shifting of C1 and 2 of nitrile groups. Other carbon signals are annotated in the graph. Thus, the characterization study certifies that the proposed phthalonitrile oligomers were successfully synthesized.

Thermal cure behaviour

The thermal properties of the oligomeric PBP-Phs were studied using a DSC instrument (Fig. 1). All the oligomers separately exhibit a distinct T_g ranging from 98 °C to 238 °C, increasing as the molar weights of the PBP-Phs increase. These values are all lower than that of polymer PAEP with similar structure reported by Matsuo (241 °C),[23a] certifying an oligomeric nature. After T_g, an endothermic peak (211-277 °C), attributed to the fusion of the oligomer, appears in each DSC profile except PBP-Ph15. The melting transition would be a benefit for their process. On account of the high molar weight, PBP-Ph15 did not exhibit distinct molten state when heated, which would restrict its further application.

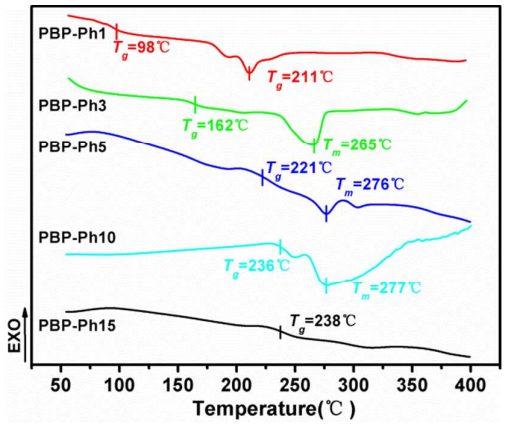

Fig. 1 DSC curves of oligomer PBP-Phs in N_2 atmosphere. PBP-Ph1-3: at the heating rate of 10 °C/min; PBP-Ph5-15: at the heating rate of 20 °C/min.

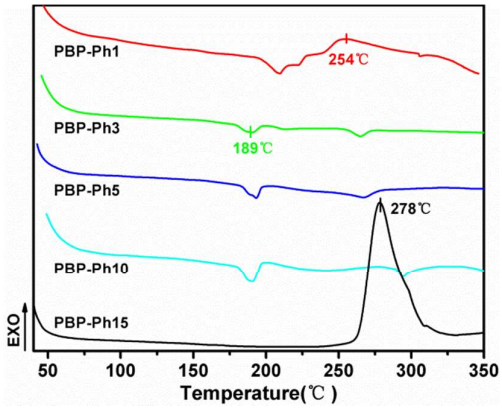

Fig. 2 DSC curves of oligomer PBP-Phs with 5 wt % BAPS in N_2 atmosphere at the heating rate of 10 °C/min.

Furthermore, the addition of curing agent is favourable to the curing of PN resins.[7b] Based on our previous work,[24] the inclusion of typically used diamine, BAPS, would result in prominent effects on the thermal properties of the phenyl-*s*-triazine-containing PN networks. As an extended work described herein, BAPS of 5 wt % addition was used to accelerate the curing of PBP-Phs. DSC instrument was resorted to investigate their curing progress (Fig. 2). In the DSC profiles of PBP-Ph1/BAPS and PBP-Ph15/BAPS hybrids, a distinct exothermic peak appears at 254 °C and 278 °C, respectively, stemmed from the reaction between the oligomer and BAPS. Whereas in the curves of PBP-Ph3-10/BAPS mixtures, no exothermic peak but sharply decreasing melting peaks, accompanied by the melting temperature migrating to higher temperature, were monitored as compared with the DSC curves of neat resins. This is possibly caused by a counteractive heat balance between melting and curing. The results above evidently demonstrate the reactivity between PBP-Phs and BAPS.

Meltability and processability

Having confirmed the reacting possible between PBP-Phs and BAPS, we subsequently investigated their processability *via* the rheologic measurement (the rheologic parameters of PBP-Phs were gathered in Table S1). The viscosities of neat PBP-Ph1-10, displayed as a function of temperature (Fig. 3), decrease dramatically on melting, and reach lower than 100 Pa·s at 218, 275, 316, and 325 °C, respectively. These temperature increases with the molecular weight of PBP-Ph. With the addition of BAPS (5 wt %), the viscosities of the systems exhibit similar behaviour at the initial stage, and then rose with the polymerization time (Fig. 4). Note that the increasing tendency of PBP-Ph3-10 blends is not so dramatic as that of PBP-Ph1 blend, probably resulted from their high melting temperatures which made them lag in melting and the following curing. However, the curing reaction could be substantiated by the isothermal rheometric measurement at 280 °C (Fig. 5). The complex viscosities of the hybrids all increase potently after the appearance of gelation at 9.3, 7.3, 5.9, and 3.9 minutes for PBP-Ph1-10/BAPS blends, respectively. The reduction of gel times indicates that there is a processing advantage when the PBP-Ph oligomers possess a short main-chain length. As anticipated, the study of the rheological behaviour shows the processability of PBP-Ph/BAPS blends, and will benefit their processing through molding and lamination technology.

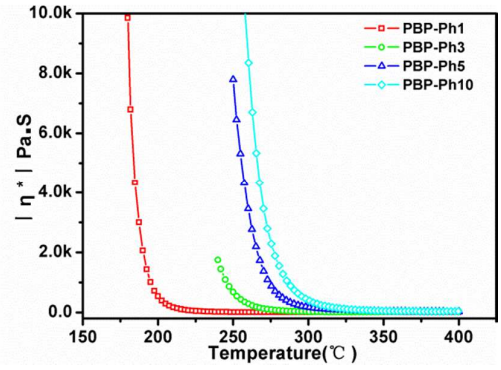

Fig. 3 Complex viscosity (η*) of neat PBP-Phs as a function of temperature at a heating rate of 3 °C/min.

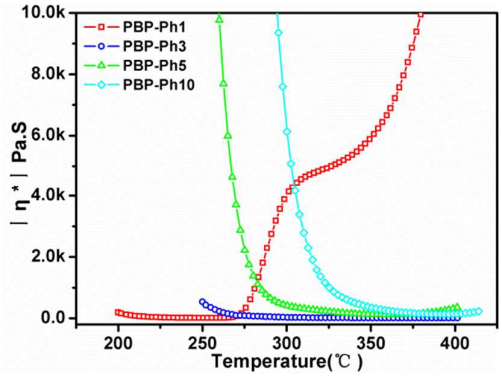

Fig. 4 Complex viscosity (η*) of PBP-Ph/BAPS blends as a function of temperature at a heating rate of 3 °C/min.

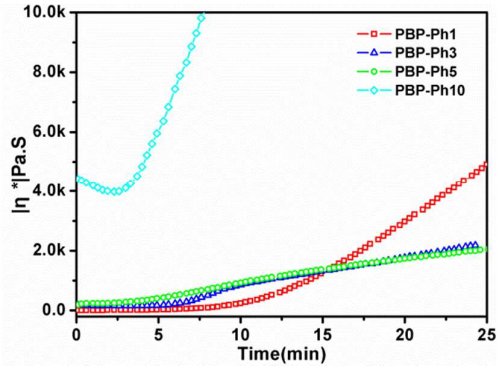

Fig. 5. Complex viscosity (η*) of PBP-Ph/BAPS blends as a function of time at 280 °C.

Thermal and thermo-oxidative stability

Our precedent work has optimized the curing procedure of PBP-Ph1/BAPS blend, and prepared a series of thermosets with high T_g, $T_{5\%d}$, and flexural strength.[24] Herein, with the aid of this curing procedure consisting of 250 °C/3 h, 285 °C/1 h, 325 °C/3 h, 350 °C/2 h, and 375 °C/8 h steps with 5 wt % BAPS, a bunch of black, vitreous polymers (Th-PBPs) were prepared. Their thermal and thermo-oxidative stability was studied with a TGA instrument under N_2 (Fig. 6) and air (Fig. 7) atmosphere, respectively. The relevant data were collected in Table S2. Th-PBPs show the weight retention temperatures of 95 % from 538 °C to 582 °C in N_2, and from 543 °C to 575 °C in air, which increase on the aromatic ether main-chain lengths in the polymer structures. The result indicates that the oligomeric spacers, constituted by both the thermally stable phenyl-*s*-triazine and biphenyl groups, are advantageous for the structural integrity of the networks against thermal decomposition. As a result, the $T_{d5\%}$s of Th-PBPs are higher than those of many cured PN networks, such as poly(aryl ether)-based oligomers (*e.g.*, PAEK-CN,[27] PEN-t-BAPh,[16b] 2CN-o-PEEK,[28] and several oligomers reported by Keller[4f, 16a, 29]), bisphthalonitrile monomers (*e.g.*, BDS,[30] BPh, BAPh, 6FPH,[14a] RPh,[13a] and monomers **1-3**[14c]), and self-curable monomers (*e.g.*, 2O-P,[31] 3a-b,[14b] and 4O-M[4b]) (The thermal data of the networks in comparison are summarized in Table S3).

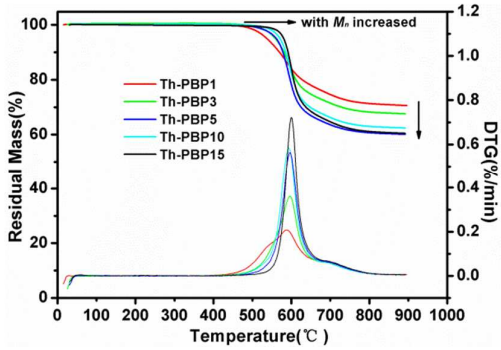

Fig. 6 TGA and DTG thermograms of Th-PBPs under N_2 atmosphere.

On the other hand, Th-PBP polymers retained 61-71% of their original masses, when heated to 900 °C in N_2. An increasing molar weight of the oligomer would likely lead to a reduction in the char yield of the network, which is contrary to the change trend of $T_{d5\%}$. This could be interpreted as a consequence of the decreasing cross-linking densities, in that the phthalocyanine or triazine contents in the corresponding network backbones lower, in turn to cause a deduction of polymer stabilities. The DTG curves indicate that the decomposition for all Th-PBPs during heating maximizes at around 590 °C under N_2 atmosphere. The peaks strengthen on the increase of the main-chain lengths, attributed to the breakage and decay of oligomeric main-chain linkage.

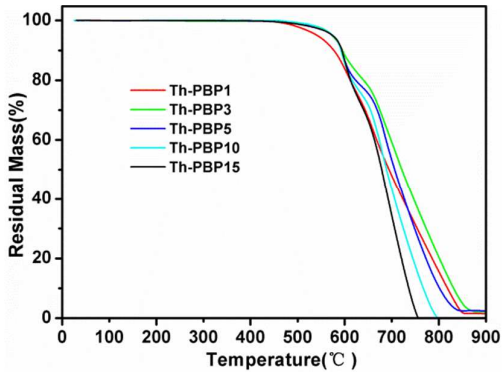

Fig. 7 TGA thermograms of Th-PBPs in air.

We further investigated the oxidative stabilities of Th-PBPs *via* disposing them at various temperatures (to a maximum of 450 °C) each for 8-h interval under ambient atmosphere (Fig. 11). After approximately 60-h period treatment, Th-PBP1-15 retained 63, 61, 53, 52, and 58 % of its initial weight, respectively. Specifically, all the samples lost weight for less than 1% after dwelling at 375 °C, and less than 10% after dwelling at 425 °C, demonstrating excellent thermal resistance again. Such property could be roughly comparable to that of the famous PMR-Ⅱ-30/Celion 6000 composite, which has a 12.5 % cumulative weight loss after aged at 371 °C for 200 h[32]. Moreover, the oxidative stabilities of PBP-Phs are intimately depending on both the length of the aromatic ether chain and the cross-linking density of the network. The chain length would have advantageous to the stability before 400 °C, and the

cross-linking density would benefit the stability at 450 °C. The interesting result would be meaningful for us to promote the heat-resistance grade of PN resins.

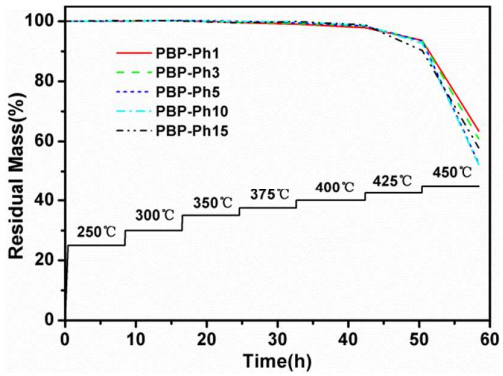

Fig. 8 Oxidative aging of Th-PBPs heated from 250 °C to 450 °C in 8-h temperature segments under ambient atmosphere.

Water absorption capability

Another well-known merit of PN thermosets is their limited water absorption capability. The relevant water uptake of Th-PBPs was studied by the guidance of ASTM D570-98 standard with samples immersed in distilled water at ambient temperature (Table 3). The amounts of absorbed water for Th-PBP1-15 after a 24-h immersion were from 0.15 wt % to 1.16 wt %, and the maximum values at equilibrium were from 1.72 wt % to 8.32 wt %. The values of water uptake of Th-PBPs increase linearly with the aromatic ether chain lengths contained in Th-PBP backbones, due to a hindrance, provided by the cross-linkage, against water permeation weakens. In addition, the absence of hydrophilic units in the polymer structures contributes to the limited water absorption of Th-PBPs as well, the property which, would be favourable to the applications under high-humidity or aqueous conditions.

Table 3 Water absorption of Th-PBPs.

Sample	Water absorption[a](%)	Water absorption[b](%)
Th-PBP1	0.15	1.72
Th-PBP3	0.19	2.07
Th-PBP5	0.51	5.45
Th-PBP10	0.55	6.72
Th-PBP15	1.16	8.32

a: Water absorption after soaking the samples in room-temperature water for 24 h. b: Saturated water absorption after soaking the samples in room-temperature water.

Mechanical properties of CF/Th-PBP laminates

Dynamic mechanical analysis (DMA) was performed to evaluate the thermal properties of T300/Th-PBP carbon fabric laminates. The temperature dependence of the storage modulus (E') and mechanical tan δ is given in Fig. 9ab. The dynamic mechanical scan displayed a tan δ peak at approximately 400, 349, 302, 298, and 294 °C for T300/Th-PBP1-15 laminates, respectively. The T_gs of Th-PBPs determined from tan δ of their fiber laminates are at least 53 °C higher than that of the high M_w PAEP (T_g, 241 °C) with a similar structure.[23a] The cross-linking sites provided by the PN unit primarily contribute to this elevation. Nevertheless, the T_gs of Th-PBPs decrease significantly as the M_ns of PBP-Ph precursors increase, implying that a longer main-chain in the backbone is not favourable to improve the T_g of PN resin. In addition, the tan δ profile of Th-PBP1 laminate exhibits the smallest scale, and hasn't reached its maximum value during the entire measurement. However, the loss modulus peaks at 385 °C (Fig. S7), implying the glass transition would occur immediately, thus, 400 °C was deemed as the softening point of Th-PBP1. The value is higher than that of many poly(aryl ether)-based PN resins,[27-28, 33] indicating that the high-stiff phenyl-*s*-triazine moiety strongly restricts the chain motion, the effect which, would result in an improvement of T_g.

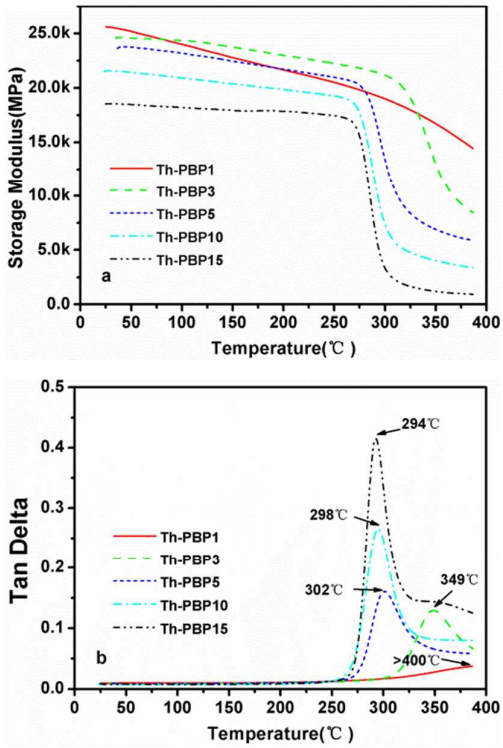

Fig. 9 DMA traces of T300/Th-PBP laminates at the heating rate of 3 °C/min. a:storage modulus versus temperature; b: tan delta versus temperature.

Afterwards, we fabricated the unidirectional CF (T700) reinforced Th-PBP composite laminates (CF/Th-PBPs) *via* solution impregnating technology, and then evaluated their flexural strength and interlaminar shear strength according to ASTM D790M and ISO 14130 standard, respectively (Fig. 10-11). From CF/Th-PBP1 to CF/Th-PBP5 (Fig. 10a), the mechanical property appears to increase progressively in terms of the value of their flexural strength (1722 MPa-1855 MPa), attributed to the increasing toughness imposed by the long main-chain length. But for CF/Th-PBP10, the flexural strength has a step decrease to 1339 MPa, originated from the suffering processability of PBP-Ph10 oligomer. The flexural modulus for CF/Th-PBPs is from 164 GPa to 113 GPa (Fig. 10b), decreasing as the molar weight of PBP-Phs increases. All the laminates possess the interlaminar shear strength higher than 71

MPa, indicative of a strong adhesive force, stemmed from the Th-PBP resins, between the neighbouring layers.

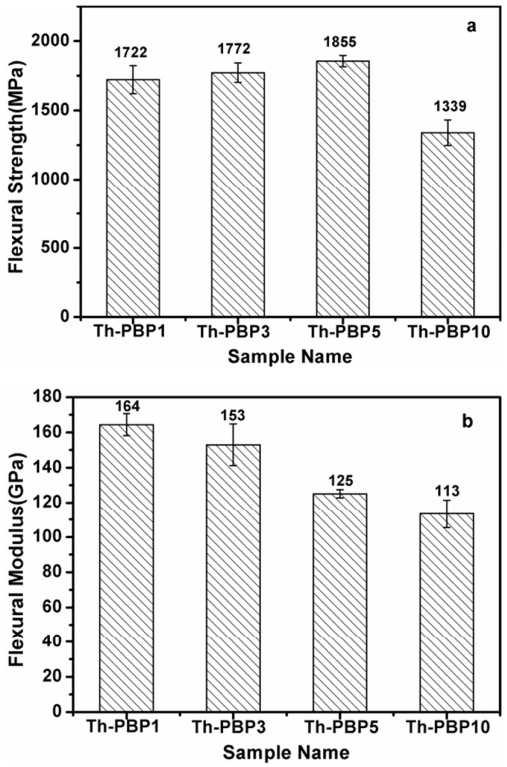

Fig. 10. Flexural strength (a) and modulus (b) of CF/Th-PBP laminates at ambient temperature.

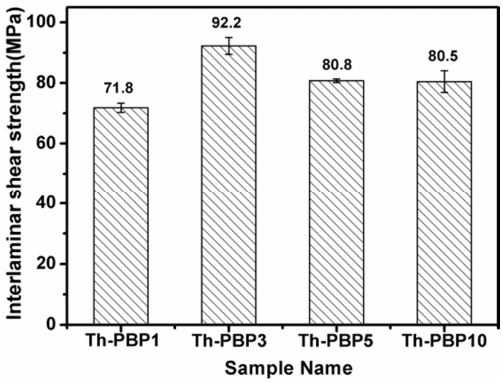

Fig. 11 Interlaminar shear strength of CF/Th-PBP laminates at ambient temperature.

Additionally, the failure mechanism was assessed by monitoring the cracked surfaces of the laminates with a scanning electron microscopy (SEM) instrument (Fig. 12). As seen in the images, the failure fashion could be classified into two categories: brittle fracture (blue pane) and coarse fracture (red pane). Brittle fracture preforms to decrease as the value of *n* increases (from a to d), confirming that the increasing aromatic ether main-chain length is beneficial to the toughness of the composites. Simultaneously, the CF pull-out could be recognized (white pane), and the matrix surface is smooth, indicating a weak fiber/matrix interface. It would inhibit proper stress transfer from the matrix to the fibers, consequently reducing the mechanical property of the laminates. Thus, more research is required to modify the fiber/matrix interface in purpose to promote the mechanical performance of the composites.

Taken together, the findings of this research demonstrate the feasibility of introducing the rigid, thermally stable moieties into the PN polymer backbones to tailor their properties. The resulting PN polymers would be qualified for applications such as structural components, adhesives, and packing materials in harsh environment.

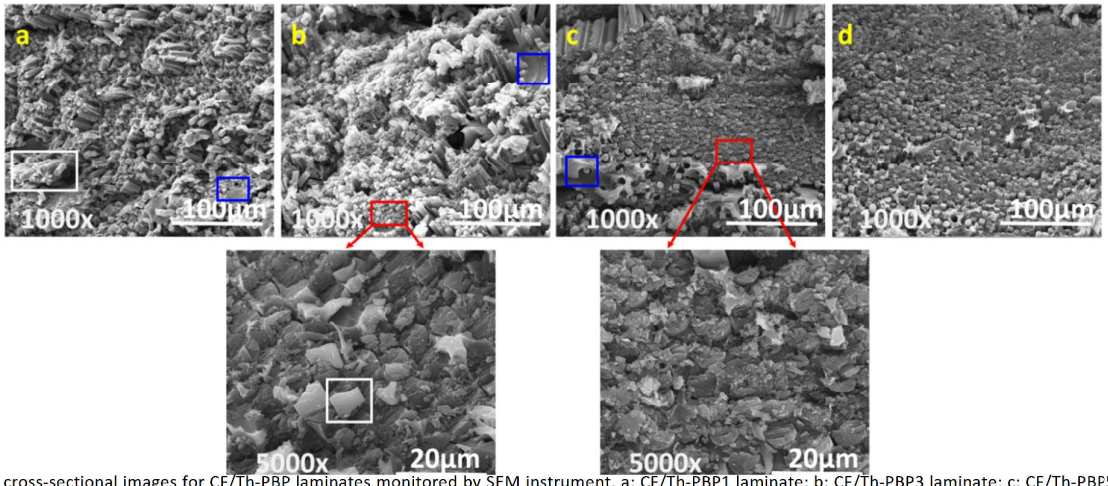

Fig. 12 The cross-sectional images for CF/Th-PBP laminates monitored by SEM instrument. a: CF/Th-PBP1 laminate; b: CF/Th-PBP3 laminate; c: CF/Th-PBP5 laminate; d: CF/Th-PBP10 laminate.

Conclusions

In this paper, we prepared a series of phenyl-*s*-triazine-containing PN resins (PBP-Phs) possessing multiple molecular weights, subsequently discussed their cross-linking, processibility, physical properties, and advanced application for CF reinforced composites. Bis[4-(4-aminophenoxy)phenyl]sulfone (5 wt %) was employed to co-cure with PBP-Phs, and the viscosity parameters of the blend system can be controlled as a function of the oligomer molar weights and the curing conditions. When fully cured, owing to the presence of phenyl-s-triazine units in the polymer main-chain, Th-PBP polymers exhibit excellent thermal and thermal-oxidative stabilities, compared with many other PN counterparts. Meanwhile, they also display limited water uptake capacities, and their CF reinforced laminates exhibit commendable thermal and mechanical properties. All the properties of Th-PBPs or their reinforced composites are intimately related to the molecular weights of the PBP-Ph precursors. Because of the merits displayed above, we would certainly suggest the phenyl-*s*-triazine-bearing PN polymers (Th-PBPs) applied as candidate matrices for high-temperature structural or functional components in aerospace, marine, and military fabrication fields.

Acknowledgments

We thank the National HighTechnology Research and Development Program ("863"Program) of China (Nos. 2015AA033802) and the National Science Foundation of China (Nos. 21074017).

Notes and references

1. (a) T. Agag, J. Liu, R. Graf, H. W. Spiess and H. Ishida, *Macromolecules*, 2012, **45**, 8991-8997; (b) I. Hamerton, L. T. McNamara, B. J. Howlin, P. A. Smith, P. Cross and S. Ward, *Macromolecules*, 2014, **47**, 1935-1945.
2. (a) P. M. Hergenrother, *High Perform. Polym.* , 2003, **15**, 3-45; (b) Y. Liu, Y. Zhang, Q. Lan, S. Liu, Z. Qin, L. Chen, C. Zhao, Z. Chi, J. Xu and J. Economy, *Chem. Mater.* , 2001, **24**, 1212-1222; (c) W. Y. Huang and S. Y. Huang, *Macromolecules*, 2010, **43**, 10355-10365.
3. (a) D. M. Wu, Y. C. Zhao, K. Zeng and G. Yang, *J. Polym. Sci., Part A: Polym. Chem.* , 2012, **50**, 4977-4982; (b) X. Q. Zou, M. Z. Xu, K. Jia and X. B. Liu, *J. Appl. Polym. Sci.* , 2014, **131**, 41203-41209; (c) K. Zeng, Y. Zou and G. Yang, *Des. Monomers Polym.* , 2014, **17**, 186-193; (d) J. Hu, Y. Liu, Y. Jiao, S. Ji, R. Sun, P. Yuan, K. Zeng, X. Pu and G. Yang, *RSC Adv.* , 2015, **5**, 16199-16206; (e) P. Yuan, Y. Liu, K. Zeng and G. Yang, *Des. Monomers Polym.* , 2015, **18**, 343-349.
4. (a) D. D. Dominguez and T. M. Keller, *Polymer*, 2007, **48**, 91-97; (b) B. Amir, H. Zhou, F. Liu and H. Aurangzeb, *J. Polym. Sci., Part A: Polym. Chem.* , 2010, **48**, 5916-5920; (c) M. Laskoski, A. Neal, T. M. Keller, D. Dominguez, C. A. Klug and A. P. Saab, *J. Polym. Sci., Part A: Polym. Chem.* , 2014, **52**, 1662-1668; (d) Y. Zhan, X. Yang, H. Guo, J. Yang, F. Meng and X. Liu, *J. Mater. Chem.* , 2012, **22**, 5602-5608; (e) H. Guo, Y. Zhan, Z. Chen, F. Meng, J. Wei and X. Liu, *J. Mater. Chem. A* 2013, **1**, 2286-2296; (f) M. Laskoski, D. D. Dominguez and T. M. Keller, *J. Polym. Sci., Part A: Polym. Chem.* , 2013, **51**, 4774-4778.
5. C. S. Marvel and J. H. Rassweiler, *J. Am. Chem. Soc.* , 1958, **80**, 1197-1199.
6. (a) T. M. Keller and J. R. Griffith, *Abstr. Pap. Am. Chem. S.*, 1978, **176**, 105-106; (b) T. M. Keller and J. R. Griffith, *J. Fluorine Chem.* , 1979, **13**, 315-324.
7. (a) T. M. Keller, T. R. Price and J. R. Griffith, *Abstr. Pap. Am. Chem. S.*, 1980, **180**, 165-166; (b) T. M. Keller and T. R. Price, *J. Macromol. Sci. A*, 1982, **A18**, 931-937; (c) S. B. Sastri and T. M. Keller, *J. Polym. Sci., Part A: Polym. Chem.* , 1998, **36**, 1885-1890.
8. (a) R. P. Linstead and A. R. Lowe, *J. Chem. Soc.* , 1934, 1022-1027; (b) T. R. Walton and J. R. Griffith, *Abstr. Pap. Am. Chem. S.*, 1975, 98-99.
9. Y. Z. Meng, I. A. Abu-Yousef, A. R. Hlil and A. S. Hay, *Macromolecules*, 2000, **33**, 9185-9191.
10. (a) A. W. Snow, J. R. Griffith and N. P. Marullo, *Macromolecules*, 1984, **17**, 1614-1624; (b) K. Zeng, K. Zhou, S. Zhou, H. Hong, H. Zhou, Y. Wang, P. Miao and G. Yang, *Eur. Polym. J.* , 2009, **45**, 1328-1335; (c) Z. Chen, X. Yang, M. Xu and X. Liu, *High Perform. Polym.* , 2013, **26**, 3-11.
11. (a) P. J. Burchill, *J. Polym. Sci., Part A: Polym. Chem.* , 1994, **32**, 1-8; (b) H. Sheng, X. Peng, H. Guo, X. Yu, C. Tang, X. Qu and Q. Zhang, *Mater. Chem. Phys.* , 2013, **142**, 740-747.
12. D. Augustine, D. Mathew and C. P. Reghunadhan Nair, *Polymer*, 2015, **60**, 308-317.
13. (a) T. M. Keller and D. D. Dominguez, *Polymer*, 2005, **46**, 4614-4618; (b) D. D. Domiguez and T. M. Keller, *High Perform. Polym.* , 2006, **18**, 283-304.
14. (a) S. B. Sastri and T. M. Keller, *J. Polym. Sci., Part A: Polym. Chem.* , 1999, **37**, 2105-2111; (b) A. Badshah, M. R. Kessler, H. Zhou, J. H. Zaidi, S. Hameed and A. Hasan, *Polym. Chem.* , 2013, **4**, 3617-3622; (c) A. Badshah, M. R. Kessler, H. Zhou and A. Hasan, *Polym. Int.* , 2014, **63**, 465-469.
15. H. Zhou, A. Badashah, Z. Luo, F. Liu and T. Zhao, *Polym. Adv. Technol.* , 2011, **22**, 1459-1465.
16. (a) M. Laskoski, D. D. Dominguez and T. M. Keller, *Polymer*, 2007, **48**, 6234-6240; (b) R. Du, W. Li and X. Liu, *Polym. Degrad. Stab.* , 2009, **94**, 2178-2183.
17. (a) S. B. Sastri, J. P. Armistead and T. M. Keller, *Polym. Compos.* , 1996, **17**, 816-822; (b) S. B. Sastri, J. P. Armistead, T. M. Keller and U. Sorathia, *Polym. Compos.* , 1997, **18**, 48-54.
18. T. M. Keller, *J. Polym. Sci., Part A: Polym. Chem.* , 1987, **25**, 2569-2576.

19. (a) M. Xu, X. Shi, X. Zou, H. Pan, M. Liu, K. Jia and X. Liu, *J. Magn. Magn. Mater.* , 2014, **371**, 20-28; (b) L. F. Tong, Z. J. Pu, Z. R. Chen, X. Huang and X. B. Liu, *Polym. Compos.* , 2014, **35**, 344-350; (c) M. Liu, K. Jia and X. Liu, *J. Appl. Polym. Sci.* , 2015, **132**, 41595-41602; (d) T. M. Robert, D. Augustine, S. M. Chandran, D. Mathew and C. P. R. Nair, *RSC Adv.* , 2015, **5**, 1198-1204; (e) K. Jia, P. Wang, L. Yuan, X. Zhou, W. Chen and X. Liu, *J. Mater. Chem. C*, 2015, **3**, 3522-3529; (f) F. Meng and X. Liu, *RSC Adv.* , 2015, **5**, 7018-7022.
20. F. Zhao, R. Liu, C. Kang, X. Yu, K. Naito, X. Qu and Q. Zhang, *RSC Adv.* , 2014, **4**, 8383-8390.
21. (a) G. P. Yu, J. Y. Wang, C. Liu, E. C. Lin and X. G. Jian, *Polymer*, 2009, **50**, 1700-1708; (b) G. P. Yu, J. Y. Wang, C. Liu, E. C. Lin and X. G. Jian, *Polymer*, 2009, **50**, 1700-1708; (c) G. P. Yu, C. Liu, J. Y. Wang, G. H. Li, Y. J. Han and X. G. Jian, *Polymer*, 2010, **51**, 100-109; (d) G. P. Yu, C. Liu, X. P. Li, J. Y. Wang, X. G. Jian and C. Y. Pan, *Polym. Chem.* , 2012, **3**, 1024-1032; (e) C. Liu, J. Y. Wang, E. C. Lin, L. S. Zong and X. G. Jian, *Polym. Degrad. Stab.* , 2012, **97**, 460-468.
22. (a) D. M. Tigelaar, A. E. Palker, C. M. Jackson, K. M. Anderson, J. Wainright and R. F. Savinell, *Macromolecules*, 2009, **42**, 1888-1896; (b) D. M. Tigelaar, A. E. Palker, R. H. He, D. A. Scheiman, T. Petek, R. Savinell and M. Yoonessi, *J. Membr. Sci.* , 2011, **369**, 455-465.
23. (a) S. Matsuo, *J. Polym. Sci., Part A: Polym. Chem.* , 1994, **32**, 2093-2098; (b) R. Fink, C. Frenz, M. Thelakkat and H. W. Schmidt, *Macromolecules*, 1997, **30**, 8177-8181; (c) R. Fink, Y. Heischkel, M. Thelakkat, H. W. Schmidt, C. Jonda and M. Huppauff, *Chem. Mater.* , 1998, **10**, 3620-3625.
24. L. S. Zong, C. Liu, S. H. Zhang, J. Y. Wang and X. G. Jian, *Submitted to Polymer*, 2015, Unpublished data.
25. M. Barikani and S. Mehdipour–Ataei, *J. Polym. Sci., Part A: Polym. Chem.* , 2000, **38**, 1487-1492.
26. R. Singh and A. S. Hay, *Macromolecules*, 1992, **25**, 1025-1032.
27. T. Liu, Y. Yang, T. Wang, H. Wang, H. Zhang, Y. Su and Z. Jiang, *Polym. Eng. Sci.* , 2014, **54**, 1695-1703.
28. H. Zhang, T. Liu, W. Yan, Y. Su, H. Yu, Y. Yang and Z. Jiang, *High Perform. Polym.* , 2014, **26**, 1007-1014.
29. (a) T. M. Keller, *Chem. Mater.* , 1994, **6**, 302-305; (b) D. D. Dominguez and T. M. Keller, *High Perform. Polym.* , 2006, **18**, 283-304.
30. X. Peng, H. Sheng, H. Guo, K. Naito, X. Yu, H. Ding, X. Qu and Q. Zhang, *High Perform. Polym.* , 2014, **26**, 837-845.
31. H. Zhou, A. Badashah, Z. Luo, F. Liu and T. Zhao, *Polym. Adv. Technol.* , 2011, **22**, 1459-1465.
32. R. D. Vannucci, *Sampe Quarterly-Society for the Advancement of Material and Process Engineering*, 1987, **19**, 31-36.
33. (a) Y. Zou, J. Yang, Y. Zhan, X. Yang, J. Zhong, R. Zhao and X. Liu, *J. Appl. Polym. Sci.* , 2012, **125**, 3829-3835; (b) J. Yang, X. L. Yang, Y. K. Zou, Y. Q. Zhan, R. Zhao and X. B. Liu, *J. Appl. Polym. Sci.* , 2012, **126**, 1129-1135; (c) M. Laskoski, D. D. Dominguez and T. M. Keller, *J. Polym. Sci., Part A: Polym. Chem.* , 2005, **43**, 4136-4143.

